

Effects of an Inhomogeneous Concentration Distribution on Rate Constants of Radical Reactions in Liquids obtained by Time-resolved and Modulation Spectroscopy

Hanns Fischer,* Henning Paul, Kurt Münger, and Tsing Dschen

Physikalisch-Chemisches Institut der Universität, Winterthurerstrasse 190, CH-8057 Zürich, Switzerland

Non-uniform concentration distributions caused by photochemical generation of radicals in solution affect kinetic responses observed in experiments using time-resolved or modulated detection. Formulas for the correct analysis of kinetic measurements are derived for various experimental conditions. It is shown that the effects are generally much smaller than stated previously by other authors, and this is verified by the results of experiments on self-termination reactions of *t*-butyl and benzyl radicals.

A large number of absolute rate constants for radical reactions in liquid solutions have been obtained mainly by the application of kinetic optical absorption or e.s.r. spectroscopy combined with pulse radiolytic or photolytic radical generation.¹⁻³ In general, the data resulted from analyses of time or frequency responses of the radical concentration on pulse, intermittent, or modulated generation according to expected rate laws. All methods of detection average over some part or the whole sample volume. The Beer-Lambert law of light absorption dictates that photolytic radical generation produces a spatially inhomogeneous radical concentration distribution in the sample. Consequently, for reactions with half-lives depending on concentration, for instance second-order self-reactions, the rates are different for different sample portions, and one may expect that the rate laws for the averaged concentrations differ from those valid for homogeneous distributions which are commonly used in the analyses.

Recently, Basu and McLauchlan⁴ presented a theoretical analysis of the effect of spatially non-uniform radical generation by pulse photolysis on second-order self-reactions. Their main conclusion was, 'once more than a few percent of the incident light is absorbed a significant deviation from true second-order behaviour is observed. Both the shape (of the time profile) and the apparent rate change ...' Now, the experimental parts of all relevant publications³ on second-order rate constants show that the stated condition of very low absorbance was never met in the past. For obvious sensitivity reasons, absorbances, where given, of $D < 0.5$ (32% absorption) were seldom applied, and they were often even larger than $D = 1$ (90% absorption). For such high values large deviations from true second-order behaviour were inferred⁴ which may have escaped detection since the signal to noise ratios of the experimental data often allowed only crude analysis by forced fits. Thus, McLauchlan's statements cast considerable doubt on the accuracy of most, if not all of the many second-order rate constants obtained with photochemical radical generation hitherto.³

However, in a quite similar theoretical treatment Leuschner, Krohn, and Dohrmann⁵ came to a totally different conclusion. They indicated that for self-reactions the effects of non-uniform radical distributions on the second-order decays are low even for absorbances corresponding to 95% absorption, and recommended this value as an optimum for time-resolved kinetic e.s.r. studies on such reactions. They also point out⁶ that the treatment of McLauchlan was technically correct, yet the results were interpreted in a misleading way, unfortunately.

This work reconsiders and extends the theory of inhomogeneity effects in more detail. We also treat influences expected for modulation spectroscopy, both on measurements of lifetimes and of CIDEP enhancements. Here, we especially refer to

the possible errors of data presented in one of our previous publications⁷ which was cited by Basu and McLauchlan⁴ as one of the 'common and recent contributions' which have 'underestimated or neglected the effect of light absorption.' In total, our extended theoretical conclusions strongly support the views of Leuschner, Krohn, and Dohrmann.⁶ They are verified by experiments on second-order rate constants obtained by time-resolved e.s.r. and on lifetimes determined by modulated optical spectroscopy.

Time-resolved Spectroscopy

Theory.—To conform with previous treatment,⁴⁻⁶ with most of the published work³ employing photochemical radical generation and with the experiments described below, this section only considers e.s.r. detection. It is common practice to produce the radicals (half-life typically in the range $200 \mu\text{s} \lesssim \tau \lesssim 3 \text{ ms}$) either by short light flashes ($t_p \ll \tau$) or by irradiation interrupted by a mechanical device.¹ In the latter case the initiation period is normally long compared with τ so that the radical concentration reaches the steady-state value. One records the e.s.r. signal, sums up over many individual cycles of radical formation and decay to improve the signal to noise ratio, and fits the time-profiles of decay to the rate laws expected from the reaction mechanism. The radical concentrations R obey equations (1) for reactions of first-order, (2) for second-order

$$R(t) = R(0)\exp(-k_1 t) \quad (1)$$

$$R(t) = R(0)[1 + 2k_2 R(0)t]^{-1} \quad (2)$$

$$R(t) = R(0)\exp(-k_1 t)[1 + 2k_2 R(0)t]^{-1} \quad (3)$$

self-reactions, and (3) for second-order self-reactions weakly perturbed by a concurrent first-order process. Relation (3) has recently been applied to appropriate systems⁸⁻¹⁰ in a slightly more general form which reduces to (3) for $k_1 \ll 2k_2 R(0)$. In the analysis, one assumes that the observed signal S is proportional to R , i.e. one applies equations (1)–(3) to $S(t)$. Calibration yields $R(0)$ from $S(0)$, so that $2k_2$ can be extracted from the first second-order lifetime $\tau = [2k_2 R(0)]^{-1}$.

As mentioned above, the method of detection averages over a finite volume of the sample, and the light absorption causes an inhomogeneous distribution of the initial radical concentration. The question to be answered is then, on how much the true decay profiles deviate from the time-dependences (1)–(3). It is immediately obvious⁴ that there will be no effects for first-order reactions since their half-lives do not depend on the concentrations. Further, the exponential term of equation (3) remains unchanged on averaging. Thus, it suffices to treat the second-order self-reaction. Further, effects of mixing by

diffusion can be neglected since for liquids the mean diffusion length in a radical lifetime is very small compared with the sample dimensions⁴⁻⁶ and with the penetration depth of the light unless very high absorbances are applied.

We treat the commonly used TE₁₀₂ e.s.r. cavity configuration in the X-band with dimensions of ca. 22 × 10 × 44 mm³ in cartesian *x, y, z*-co-ordinates. The sample is contained in a flat optical cell with inner dimensions *a* = 22 mm, *b* < 10 mm, and 0.2 ≤ *d* ≤ 4 mm in the same co-ordinate system or in a cylindrical tube with length *a* along *x* and radius *r* ≤ 2 mm. A light beam homogeneous in the *xy*-plane is incident on the sample in the *z*-direction. Inhomogeneities caused by window, cooling devices, and sample walls are ignored. The substrate with concentration *c* obeys the Beer-Lambert law with decadic absorption coefficient ϵ . For polychromatic sources ϵ is approximated by its average over the wavelength distribution. Substrate depletion shall be negligible. To avoid this important source of errors flow systems have been devised and widely used by our and other^{6,10,11} groups. At high flow rates *c* and *R* become independent of *x*, but flow effects can still be neglected⁶ since the dwell times (usually seconds) are long compared with τ . Finally, we will take it that the response times of the spectrometer and the sampling device are short compared with the radical lifetimes so that no instrumental distortions of the time-profiles occur. If not, we assume that they are properly taken into account by deconvolution.

The e.s.r. signals are then proportional to the number of radicals in the sample [relation (4)]. κ represents a sensitivity

$$S \sim \int R \kappa d\tau \quad (4)$$

factor governed by the *B*₁ field distribution. As shown by McLauchlan⁴ its influence can safely be neglected for the sample dimensions given above, so that equation (5) holds

$$S = NV\bar{R} \quad (5)$$

where *V* is the sample volume and \bar{R} the average radical concentration.

The rate of radical generation is given by equation (6) where

$$I/l \text{ mol}^{-1} \text{ s}^{-1} = 1000\phi 2.303\epsilon c Q_0 \exp(-2.303\epsilon cz) = I_0 \exp(-2.303\epsilon cz) \quad (6)$$

ϕ is the quantum yield of radical formation, *Q*₀ is the quantum flux in mol cm⁻² s⁻¹, eventually wavelength averaged, and *I*₀ is the rate at the sample surface (*z* = 0). For flash photolysis with pulse width *t*_p short compared with the radical lifetime τ , the initial concentration distribution is given by equation (7). If the

$$R(0) = I t_p \quad (7)$$

steady-state concentration is reached in the on-period of photolysis, as for the technique using intermittent radical generation, then equation (8) holds. From (6)–(8) it follows

$$R(0) = (I/2k_2)^{1/2} \quad (8)$$

immediately that for given sample dimensions in the *z*-direction the pulse method is more subject to inhomogeneity effects since the square-root in (8) reduces the *z*-dependence of *R*(0).

In the following we treat the flat cell arrangement first, define a 'surface' second-order lifetime⁴ with *R*₀(0), the initial

$$\tau_0 = [2k_2 R_0(0)]^{-1} \quad (9)$$

concentration for *z* = 0, and introduce the abbreviation (10).

$$\alpha = 2.303\epsilon cd = 2.303D \quad (10)$$

Further, we only consider the technique employing intermittent photolysis and equation (8), and note here that α has to be replaced by 2α to translate the formulas to the case of flash photolysis.

The integration (5) over the cell volume then leads to (11)

$$S(t) = NV R_0(0) \frac{1}{T_0} \frac{2}{\alpha} \ln[(1 + T_0)/(1 + T_0 e^{-\alpha/2})] \quad (11)$$

where *T*₀ = *t*/ τ ₀. This is equation (7) of Dohrmann and co-workers⁶ and, in essence, equation (8) of Basu and McLauchlan.⁴ For *T*₀ = 0 one has (12) so that equation (11) is equivalent to (13).

$$S(0) = NV R_0(0) \frac{2}{\alpha} (1 - e^{-\alpha/2}) \quad (12)$$

$$S(t) = S(0)(1 - e^{-\alpha/2})^{-1} \frac{1}{T_0} \ln[(1 + T_0)/(1 + T_0 e^{-\alpha/2})] \quad (13)$$

To determine the effect of non-uniform radical concentration Basu and McLauchlan⁴ compared equation (11) with a 'true' second-order behaviour defined by equation (14). This does in

$$S(t) = S(0)(1 + T_0)^{-1} \quad (14)$$

fact lead to gross differences as revealed by curves a–c in Figure 1. The power expansion of equation (13) valid for small α

$$S(0)(1 + T_0)^{-1} \left\{ 1 + \frac{\alpha}{4} \frac{T_0}{1 + T_0} + \frac{\alpha^2}{48} \left(\frac{T_0}{1 + T_0} \right)^2 + [\alpha^3] + \dots \right\} \quad (15)$$

is (15). Obviously, the deviations of (13) from (14) start with a term linear in α and become larger as time goes on (*T*₀ → ∞). Even for *D* = 0.1 deviations as large as 3% occur, and for *D* = 0.5 the first half-life is increased by 15%.

However, this comparison does not correspond to the usual analysis of experimental traces, where one extracts the kinetic parameters from the initial concentration and the experimental

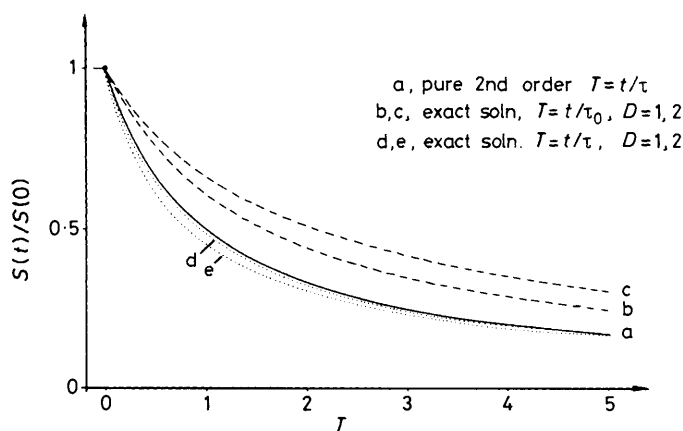


Figure 1. Effect of non-uniform radical concentration on decay profiles for a self-termination reaction: a, according to the second-order rate law with uniform concentration $\bar{R}(0)$; b, c, exact solution plotted according to equation (13) following Basu and McLauchlan,⁴ d, e, exact solution plotted according to equation (19)

half-life $\tau = [2kR(0)]^{-1}$. Since one always measures sample averages, the average $R(0)$ is used for $R(0)$ and not the unknown $R_0(0)$. Consequently, one should compare equation (13) with (16) where $T = t/\bar{\tau}$ and $\bar{\tau}$ is defined by $[2k_2\bar{R}(0)]^{-1}$. It is easy to

$$S(t) = S(0)(1 + T)^{-1} \quad (16)$$

show that for the flat cell arrangement (17) and (18) hold.

$$\bar{\tau} = \tau_0 \frac{\alpha}{2} (1 - e^{-\alpha/2})^{-1} = \tau_0 f(\alpha) \quad (17)$$

$$\bar{R}(0) = (I_0/2k_2)^{1/2} [f(\alpha)]^{-1} = R_0(0) [f(\alpha)]^{-1} \quad (18)$$

Replacement of τ_0 in (13) by $\bar{\tau}$ yields equation (19), a form

$$S(t) = S(0) \frac{2}{\alpha} \frac{1}{T} \ln \left[\frac{1 + fT}{1 + fTe^{-\alpha/2}} \right] \quad (19)$$

which should be compared with (16). This comparison can be made by inspection of curves a, d, and e of Figure 1. Obviously, even for substantial absorbances the exact solution yields decay profiles which are hardly distinguishable from the second-order decays valid for the average concentration uniformly dispersed over the sample. Moreover the deviations decrease with increasing time. This is very reasonable since the decrease of second-order lifetimes $(2kR)^{-1}$ with increasing R must average out the initial inhomogeneity as time evolves. Apparently, this went unnoticed before.⁴ The power expansion of equation (19) is (20). The deviations from (16) start with a term quadratic in α ,

$$S(t) = S(0)(1 + T)^{-1} \left[1 - \frac{\alpha^2}{48} \frac{T}{(1 + T)^2} + [\alpha^4] - \dots \right] \quad (20)$$

and (20) again demonstrates that they decrease with increasing time for $T > 1$.

Numerical calculations for the time range $0 \leq t \leq 5\bar{\tau}$ show that the differences between the exact solution (19) and the second-order law (16) amount to $< 2\%$ for $D \leq 1$. Further, least-squares fits of equation (16) to the exact solution were carried out treating $S(0)$ and $\bar{\tau}$ as fit parameters. The results are given in Table 1, and may be used as correction factors. Since the deviations decrease with time it is advisable to discard early portions of the decay profiles if signal to noise permits since then better values of $\bar{\tau}$ result. Figure 2 displays the exact time

profile for $D = 2$ and its least-squares fit to equation (16). Visually the fit is agreeable though it should be noticed that the second-order function decays slower than the exact solution for short times but slightly faster for long times.

Since many authors^{1,12-16} have used cylindrical sample tubes the above calculations were also carried out for this condition, again neglecting effects of substrate depletion and treating the case of intermittent radical generation with $R(0)$ given by the steady-state value. We now use the abbreviation (21) to describe the absorption. The average steady-state

$$\beta = 2.303\epsilon cr \quad (21)$$

concentration is then given by (22) where $I_1(\beta)$ is a Bessel

$$\bar{R}(0) = (I_0/2k_2)^{1/2} \frac{2}{\beta} [I_1(\beta) - L_1(\beta)] = R_0(0) [g(\beta)]^{-1} \quad (22)$$

function of imaginary argument and $L_1(\beta)$ is a modified Struve function. Expansions of these functions in power series are available and yield equation (23). The equation for the time-

$$[g(\beta)]^{-1} = \sum_0^{\infty} \frac{(\beta/2)^{2k}}{k!(k+1)!} - \frac{4\beta}{\pi} \sum_0^{\infty} \frac{\beta^{2k}}{(2k+1)!(2k+3)!!} \quad (23)$$

dependent signal corresponding to (19) becomes (24) where

$$S(t) = S(0) \frac{4g}{\pi} \int_0^1 \frac{\exp(-\beta x)}{1 + gT \exp(-\beta x)} (1 - x^2)^{1/2} dx \quad (24)$$

$S(0) = NV\bar{R}(0)$ and $T = t/\bar{\tau}$ with $\bar{\tau} = [2k\bar{R}(0)]^{-1}$ as before. The integration cannot be performed analytically. However, a power expansion valid for small β can be given in the analytic form (25). The deviations from the second-order behaviour (16)

$$S(t) = S(0)(1 + T)^{-1} \left[1 - \left(\frac{1}{4} - \frac{16}{9\pi^2} \right) \beta^2 \frac{T}{(1 + T)^2} + [\beta^4]^+ \dots \right] \quad (25)$$

start again with a term quadratic in the absorption parameter β and decrease as time elapses. For a few values of β equation (24) was evaluated and least-squares fits of equation (16) to the resulting decay profiles were performed. For $\beta = 1, 2,$ and 5 one obtained in the time range of fit $0 < t \leq 5\bar{\tau}$ $\tau^F/\bar{\tau} = 0.97, 0.92,$ and 0.67 and $S^F(0)/S(0) = 0.99, 0.99,$ and 0.97 , respectively. Though a direct comparison with the effects found for the flat cell arrangement cannot be made they appear to be of

Table 1. The effect of inhomogeneous radical generation on kinetic parameters obtained by fits to a second-order rate law represented as ratios of parameters obtained from fits $[\tau^F, S^F(0)]$ to true values

Absorbance $D = \epsilon cd^b$	$0 < t < 5\bar{\tau}^a$		$\bar{\tau} < t < 5\bar{\tau}^a$	
	$\tau^F/\bar{\tau}$	$S^F(0)/S(0)$	$\tau^F/\bar{\tau}$	$S^F(0)/S(0)$
0.3	1.00 ^c	1.00	1.00	1.00
0.5	0.99	1.00	1.00	0.99
0.8	0.98	1.00	1.01	0.97
1.0	0.96	0.99	1.02	0.96
1.5	0.93	0.99	1.05	0.91
2.0	0.88	0.98	1.09	0.86
3.0	0.76	0.97	1.14	0.76
4.0	0.64	0.97	1.12	0.68
5.0	0.54	0.97	1.08	0.62

^a Time range of fit. ^b Flat cell arrangement. ^c The data in this column have also been presented by Dohrmann and co-workers.⁶

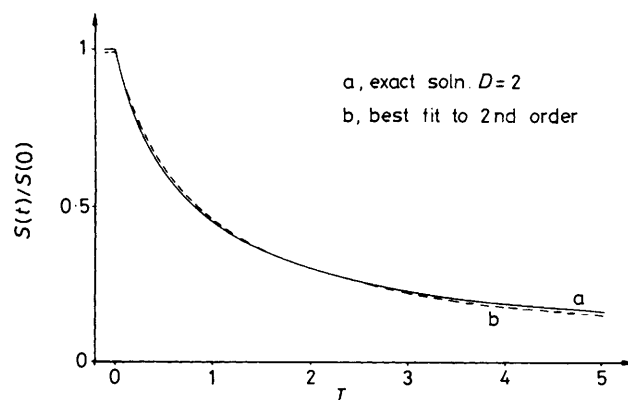


Figure 2. Comparison of the exact solution for $D = 2$ with its least-squares fit to the second-order rate law

Table 2. Concentrations, second-order lifetimes, and rate constants of self-termination for t-butyl radicals in n-octane at various absorbances

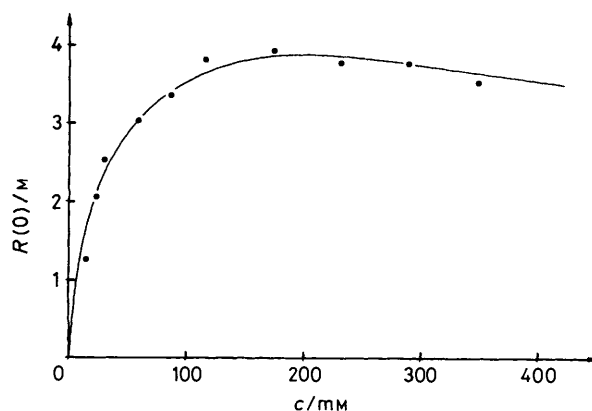
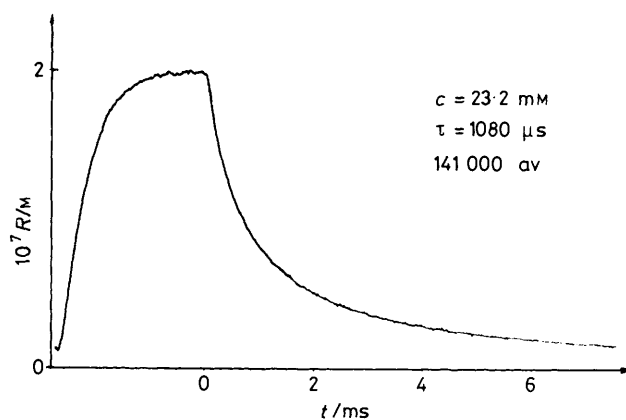
c/mm	D	$10^7 \overline{R(0)}/M$	$\bar{\tau}/\mu\text{s}$	$2 \times 10^9 k_2 / \text{l mol}^{-1} \text{s}^{-1}$
14.5	0.081	1.27 ^a	1 870 ^a	4.2 ^b
23.2	0.13	2.07	1 080	4.5
29.0	0.16	2.54	920	4.3
58.0	0.32	3.06	780	4.2
87.0	0.48	3.35	740	4.0
116	0.65	3.83	660	4.0
174	0.97	3.92	705	3.6
232	1.29	3.81	650	4.0
290	1.61	3.81	640	4.1
350	1.95	3.54	760	3.7

^a Averages from 2–4 individual determinations. Statistical errors of individual fits $\leq 5\%$, deviations between individual determinations using the same stock solution $\leq 3\%$. ^b Reference value, see text.

similar magnitude for similar total absorptions. For pulse photolysis β has to be replaced by 2β in the above equations.

Finally, we would like to point out the 'optimum' experimental conditions for kinetic e.s.r. experiments employing intermittent radical generation with $\overline{R(0)}$ given by equation (8). For the flat cell arrangement and a given dimension d the average radical concentration $\overline{R(0)}$ has a maximum for $1 + \alpha = \exp(\frac{2}{D})$, which leads to an 'optimum' absorbance of $D_{\text{opt}} = 1.092$. This corresponds to 92% absorption and is not far from the value recommended by Dohrmann and co-workers.⁶ For D_{opt} least-squares fits of experimental time profiles to equation (16) lead to parameters which differ by *ca.* 2% from the correct ones. For cylindrical sample tubes $\overline{R(0)}$ attains a maximum value at $\beta = 2.303\epsilon cr = 1.57$ and the differences are *ca.* 4%. For both cases $\overline{R(0)}$ and hence $S(0)$ increase sharply for low absorption and decrease only slowly for absorptions larger than the 'optimum' values.

Experimental.—To verify the results of the previous section, time-resolved e.s.r. experiments were performed using an experimental arrangement described in detail previously⁹ with some improvements regarding time response (now 20 μs) and sector frequency stability.¹⁷ t-Butyl radicals were generated by photolysis of di-t-butyl ketone in n-octane solvent at 3 °C. From previous work¹⁸ it can be seen that this method of generation supplies t-butyl radicals only which decay by a pure second-order self-reaction. A flow system with a flat cell of $d = 4$ mm was used. The wavelength region of photolysis by the u.v. light of a 1 kW Hg-Xe lamp (Hanovia 977-B-1) was narrowed to $295 \text{ nm} \leq \lambda \leq 340 \text{ nm}$ by a filter solution¹⁸ and an additional cut-off filter. From the emission spectrum of the lamp¹⁹ and the absorption spectra of ketone and filters an average decadic absorption coefficient $\epsilon = 13.9 \text{ l mol}^{-1} \text{ cm}^{-1}$ was calculated. The initial ketone concentration was varied from $c = 14.5$ to 350 mM, corresponding to absorbances varying from D 0.08 to 1.93. High flow rates were employed to minimize depletion, which is estimated to be $< 5\%$ for the lower concentrations. Concentration-time profiles were obtained following published procedures.^{9,17} To obtain second-order lifetimes $\bar{\tau}$ the decay parts were fitted to equation (16). The steady-state signal amplitudes $S(0)$ were recorded for each run and calibrated against a standard.⁹ They were converted into absolute average radical concentrations by adopting from previous work¹⁸ a rate constant of $2k_2 = 4.2 \times 10^9 \text{ l mol}^{-1} \text{ s}^{-1}$ for the present conditions and for the lowest ketone concentration employed. Thus, absolute rate constants given below are relative to this value. Table 2 shows the results. As

**Figure 3.** Average concentrations of t-butyl radicals during photolysis of di-t-butyl ketone for various ketone concentrations. Estimated errors $\pm 10\%$. Curve is least-squares fit of the data to equation (18)**Figure 4.** Time-dependence of the concentration of di-t-butyl radicals during intermittent photolysis of di-t-butyl ketone. The $M = -1/2$, $K = 3/2$ — line was followed, for which CIDEP effects are low. Absorbance $D = 0.13$. Noiseless trace corresponds to the fit to second-order decay

expected from equation (18) $\overline{R(0)}$ reaches a flat maximum near $D = 1$. Further, as predicted, the kinetic constants $2k_2$ are fairly insensitive to a variation of D . The scatter of the data is not due to inhomogeneity effects nor does it reflect the quality of the fits. Rather, we attribute it to a variety of external experimental factors, like small temperature variations between runs and fluctuations in spectrometer sensitivity over the extended period of measurements or in light flux and sector stability during individual runs. Figure 3 shows $\overline{R(0)}$ plotted against ketone concentration together with a least-squares fit to equation (18). From the fitting parameter α/c one obtains the average decadic absorption coefficient $\epsilon = 13.2 \text{ l mol}^{-1} \text{ cm}^{-1}$ which agrees with the estimate of $\epsilon = 13.9 \text{ l mol}^{-1} \text{ cm}^{-1}$. Still more gratifying are comparisons of individual decay profiles with their fits to second-order behaviour. Figure 4 was obtained with $D = 0.13$, and one cannot see deviations of the experimental trace from the fit. However, for $D = 1.93$ they are clearly visible (Figure 5), and correspond in form and magnitude to the calculated behaviour which was displayed in Figure 2.

Conclusions.—The foregoing results show unambiguously that the effects of inhomogeneous radical concentration on radical self-reaction rate constants are rather small for $D \leq 1$, a condition which was always fulfilled in our previous work

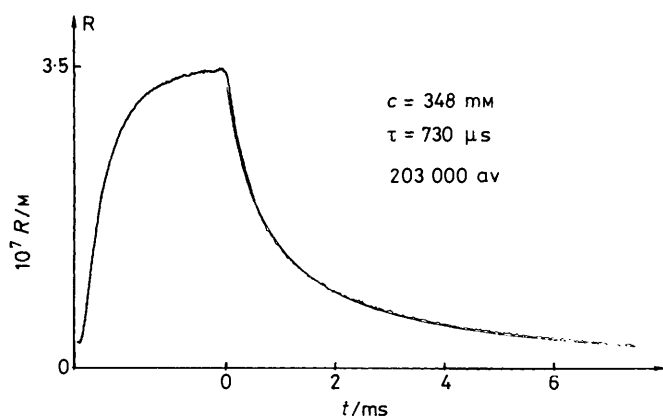


Figure 5. Same as Figure 4, except $D = 1.93$

employing time-resolved e.s.r.^{8,9,17,18,20-22} The same is very probably true for many contributions by other groups¹⁻³ though a critical evaluation cannot be made since the absorbances were, in general, not stated explicitly. There will certainly be exceptions. For instance, data obtained with absorbing substrates as solvents, such as di-*t*-butyl peroxide,^{16,23} may have to be revised in the future, though not extensively. Very likely, other effects, such as substrate depletion, or of light focusing leading to erroneous absolute radical concentrations²⁴ cause larger errors than the inhomogeneity due to the Beer-Lambert law.

For kinetics of mixed first- and second-order the inhomogeneity effects are probably similar in magnitude as for pure second order. We have claimed previously that even rather complicated kinetic schemes can be analysed from kinetic e.s.r. time profiles with signal to noise ratios similar to those of Figures 4 and 5. Several examples obtained with low absorbances ($D \lesssim 0.8$) have been given^{8,9,17,20,21} for competing reactions of second- and pseudo-first-order. The effects of mixed kinetics on the shapes of the decay profiles observed were just opposite to those expected from inhomogeneity. This, and other evidence from product distributions, confirms the validity of the previously published data.

Modulation Spectroscopy

Theory.—Modulation spectroscopy, though it yields the same kinetic information as the time-resolved one, has to be treated separately since it averages inhomogeneous radical concentrations in a different way. The harmonic modulation experiment, which has mainly been employed for the investigation of radical kinetics in solution,²⁵ applies a harmonically modulated rate of radical initiation, $I = \frac{1}{2}\hat{I}(1 + \cos\omega t)$, and monitors the resulting oscillating radical concentration [equation (26)]. For radicals vanishing by

$$R = R^{st} + A\cos(\omega t + \psi_R) \quad (26)$$

bimolecular self-reaction and a concurrent first-order process the oscillation occurs²⁶ around a time-averaged, stationary concentration [equation (27)] with amplitude (28) and phase

$$R^{st} = \frac{1}{2}\hat{I}(k_1 + 2k_2R^{st})^{-1} \quad (27)$$

$$A = \frac{1}{2}\hat{I}(\tau^{-2} + \omega^2)^{-1/2} \quad (28)$$

lag (29) where the radical lifetime τ is defined by equation (30).

$$\psi_R = -\arctan(\omega\tau) \quad (29)$$

$$\tau = (k_1 + 4k_2R^{st})^{-1} \quad (30)$$

The experiment measures A and/or ψ_R by phase-sensitive detection at ω of the e.s.r. or optical absorption signal of the radicals, and τ is commonly determined²⁵ from the frequency dependence of either the amplitude, plotting A^{-2} versus ω^2 according to equation (28), or the phase, plotting $\tan\psi_R$ versus ω according to equation (29).

In order to treat the effect of an inhomogeneous radical distribution we again consider a rectangular optical cell with a photolysis beam along the z -axis. The Beer-Lambert law of light absorption then causes R^{st} , A , and ψ_R to depend on the z -co-ordinate, and the experimentally detected oscillation is given by the z -averaged radical concentration (31). As in the time-

$$\bar{R} = \frac{1}{d} \int_0^d R^{st} dz + \frac{1}{d} \int_0^d A \cos(\omega t + \psi_R) dz \quad (31)$$

resolved measurement, it is immediately seen that the integration has no effect on the evaluation of τ from equations (28) and/or (29) as long as the radical decay obeys pure first-order kinetics. Since $\tau = 1/k_1$ and ψ_R become z -independent, the integration only replaces \hat{I} by its mean value over the sample. Therefore, we again limit the discussion to the other extreme, pure second-order decay kinetics by bimolecular radical termination. For this case, the relevant z -dependences are given by equations (32) where the subscript zero indicates the 'surface'

$$\hat{I}(z) = \hat{I}_0 \exp(-z\alpha/d) \quad (32a)$$

$$R^{st}(z) = (\hat{I}_0/4k_2)^{1/2} \exp(-\frac{1}{2}z\alpha/d) \equiv R_0^{st} \exp(-\frac{1}{2}z\alpha/d) \quad (32b)$$

$$\tau(z) = (4k_2R_0^{st})^{-1} \exp(\frac{1}{2}z\alpha/d) \equiv \tau_0 \exp(\frac{1}{2}z\alpha/d) \quad (32c)$$

values, and α is defined by equation (10). Inserting equations (28), (29), and (32) into equation (31) and performing the integrations yields (33) with average values of R^{st} and the cosine

$$\bar{R} = \bar{R}^{st} + \bar{C}\cos\omega t - \bar{S}\sin\omega t \quad (33)$$

and sine coefficients C and S given by equations (34)–(36)

$$\bar{R}^{st} = \frac{2}{\alpha}(1 - e^{-\alpha/2})R_0^{st} \quad (34)$$

$$\bar{C} = \frac{1}{\alpha}R_0^{st} \left[1 - e^{-\alpha/2} + \omega\tau_0 \arctan\left(\omega\tau_0 \frac{1 - e^{-\alpha/2}}{1 + \omega^2\tau_0^2 e^{\alpha/2}}\right) \right] \quad (35)$$

$$\bar{S} = -\frac{1}{2}\omega\tau_0 R_0^{st} \left[1 - \frac{1}{\alpha} \ln\left(\frac{1 + \omega^2\tau_0^2 e^{\alpha}}{1 + \omega^2\tau_0^2}\right) \right] \quad (36)$$

Thus, because of the finite optical density the experiment detects an average oscillation of the radical concentration with amplitude $\bar{A} = (\bar{C}^2 + \bar{S}^2)^{1/2}$ and phase lag $\bar{\psi}_R = \arctan(\bar{S}/\bar{C})$. Figure 6 shows the frequency dependences of these quantities in form of the commonly used graphs $1/\bar{A}^2$ versus ω^2 and $\tan\bar{\psi}_R$ versus ω . They are calculated from equations (34)–(36) for absorbances $D = 0.5, 1, 1.5$, and 2. \bar{R}^{st} has been kept constant and normalized to $4k_2\bar{R}^{st} \equiv \bar{\tau}^{-1} = 1$.

The broken lines in Figures 6a and b represent the fictitious limiting case of a homogeneous distribution of \bar{R}^{st} . For this situation the relations (28) and (29) are strictly valid yielding linear dependences of $1/\bar{A}^2$ on ω^2 and of $\tan\bar{\psi}_R$ on ω . Obviously, these linear relationships become increasingly violated with growing optical density and modulation frequency. This dependence on D and ω is easily seen from a power

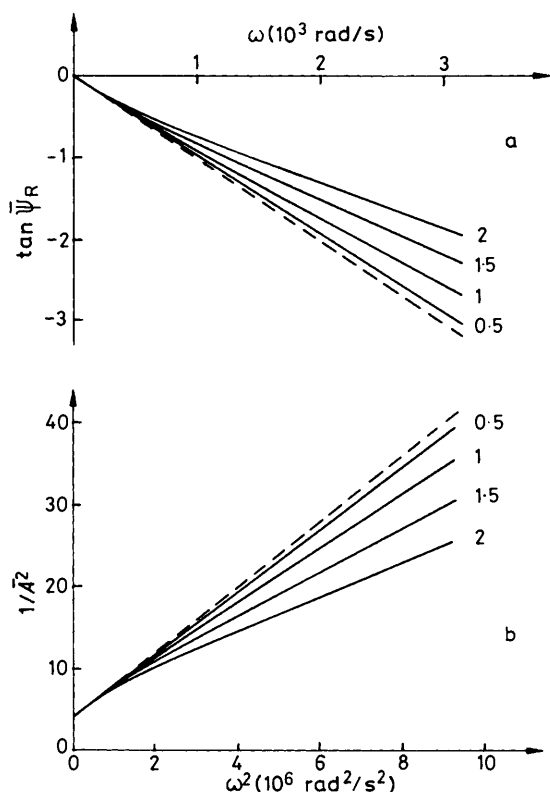


Figure 6. Effects of non-uniform radical concentration on the frequency dependences of phase shift $\bar{\psi}_R$ and amplitude \bar{A} for a self-termination reaction and absorbances $D = 0.5, 1, 1.5,$ and 2 . The broken lines refer to a uniform concentration

Table 3. Second-order lifetimes $\bar{\tau}[A]$ and $\bar{\tau}[\psi_R]$ from fits of $\bar{A}(\omega)$ and $\bar{\psi}_R(\omega)$ to equations (28) and (29) at various absorbances

D	0.2	0.5	0.8	1.0	2.0
$\bar{\tau}^F[A]$	0.99	0.96	0.90	0.86	0.65
$\bar{\tau}^F[\psi_R]$	0.99	0.96	0.90	0.85	0.63

expansion of equations (35) and (36) yielding (37) and (38). The

$$\tan \bar{\psi}_R = \frac{\bar{S}}{\bar{C}} = -\omega \bar{\tau} \left\{ 1 - \frac{1}{24} \frac{\omega^2 \bar{\tau}^2}{1 + \omega^2 \bar{\tau}^2} \alpha^2 + [\alpha^4]^{\mp} \dots \right\} \quad (37)$$

$$\bar{A}^{-2} = (\bar{S}^2 + \bar{C}^2)^{-1} = \left(\frac{2}{\bar{R}_{st}} \right)^2 (1 + \omega^2 \bar{\tau}^2) \left\{ 1 - \frac{\omega^2 \bar{\tau}^2}{24} \frac{\omega^2 \bar{\tau}^2 - 1}{(\omega^2 \bar{\tau}^2 + 1)^2} \alpha^2 + [\alpha^4]^{\mp} \dots \right\} \quad (38)$$

deviations start with terms quadratic in α , which go to a maximum value of $\alpha^2/24$ for $\omega \bar{\tau} \gg 1$. Since the modulation experiment is typically performed at frequencies $\omega \gtrsim \bar{\tau}^{-1}$ the terms in α^2 play a more significant role than the analogous term for the time-resolved experiment [compare equation (20)]. Consequently, the modulation experiment is somewhat more sensitive to inhomogeneous radical distributions. This is also demonstrated by the lifetimes $\bar{\tau}^F[A]$ and $\bar{\tau}^F[\psi_R]$ given in Table

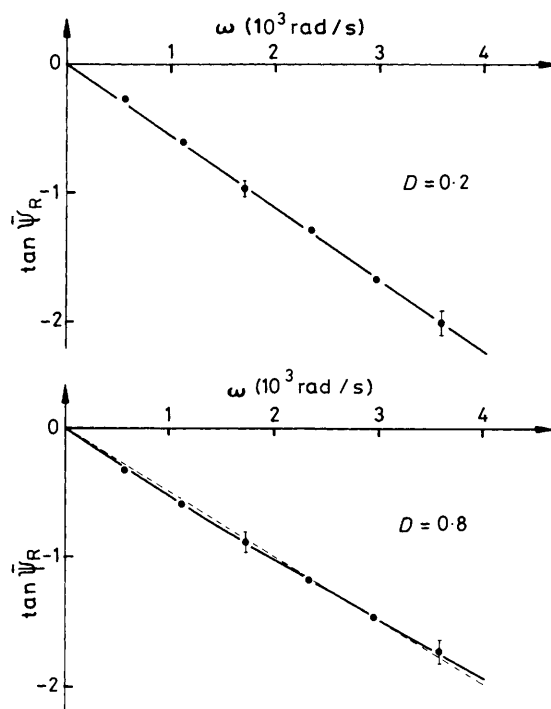


Figure 7. Frequency dependence of the phase lag $\bar{\psi}_R$ of the benzyl radical concentration during photolysis of dibenzyl ketone with absorbances $D = 0.2$ and 0.8 . Experimental points are fitted to the exact relations (35), (36) (full lines) and the approximation (29) (broken line)

3. They result if the exact frequency dependences, represented by equations (35) and (36), are analysed in the usual way by just performing 'forced' fits to $\bar{A}^{-2} \sim (1 + \omega^2 \bar{\tau}^2)$ and $\tan \bar{\psi}_R = -\omega \bar{\tau}$, thus neglecting the deviations due to the Beer-Lambert law. The values listed in Table 3 are calculated for various absorbances from linear regressions to six equally spaced points in the commonly used range $0.5 \leq \omega \bar{\tau} \leq 3$. A true mean lifetime of $\bar{\tau} = 1$ was assumed. The data obtained from the amplitude and phase show essentially equal deviations, and are already wrong by 10% at an absorbance of only $D = 0.8$.

Experimental—To verify these results we performed modulation experiments with optical detection of the oscillating radical concentration. The experimental arrangement was similar to that used previously.²⁷ For a suitable chemical system we chose the photolysis of dibenzyl ketone in cyclohexane solution at 24 °C. This system yields benzyl radicals, which decay by second-order self-reaction²⁰ and can be monitored *via* a strong absorption band at $\lambda = 316$ nm.^{27,28} A flow system with a flat quartz cell (3 and 10 mm optical pathlengths for the exciting and analysing light, respectively) was used. By means of diaphragms the diagnosing beam was limited to the inner 1 mm broad region of the 3 mm broad side of the cell. For excitation the u.v. light between $240 \lesssim \lambda \lesssim 340$ nm of a 1 kW Xe short-arc lamp (Hanovia 976 C 001) was modulated *via* the lamp current. The spectral distribution of the light and the absorption spectrum of the ketone gave an average decadic absorption coefficient $\epsilon = 370$ l mol⁻¹ cm⁻¹, which was used to adjust the desired absorbances.

Figure 7 shows the frequency dependences obtained for $\tan \bar{\psi}_R$ at optical densities 0.2 and 0.8. The points given are the experimental results corrected for small deviations, which stem from differences between equation (26) and the exact integral of

a second-order rate law containing an oscillating initiation term.^{7,26} Obviously, for $D = 0.2$ the linear relation $\tan\psi_R = -\bar{\tau}\omega$ remains a very good approximation. Linear regression and the exact fit according to equations (35) and (36) yield practically indistinguishable graphs with lifetimes $\bar{\tau}^F = (541 \pm 7)$ and $\bar{\tau} = (543 \pm 7)\mu\text{s}$, respectively. The calculation predicted (Table 3) $\bar{\tau}^F/\bar{\tau} \cong 0.99$, and that is the experimental result within the statistical error. For $D = 0.8$ there is a visible difference between the linear regression [broken line, $\bar{\tau}^F = (489 \pm 11)\mu\text{s}$] and the exact fit [full line, $\bar{\tau} = (536 \pm 13)\mu\text{s}$]. The experimental ratio $\bar{\tau}^F/\bar{\tau} \cong 0.91 \pm 0.03$ is again in good agreement with the calculated one, i.e. $\bar{\tau}^F/\bar{\tau} \cong 0.90$.

Conclusions—Calculation and experiment show the modulation method to be not quite as insensitive as the time-resolved experiment to inhomogeneous radical concentrations caused by the Beer–Lambert law of light absorption. Thus, future studies should account for the effect wherever necessary. For simple kinetic systems exhibiting decay only by bimolecular radical self-reaction this is easily done with the aid of equations (34)–(36) or (37) and (38). Modulation measurements published so far^{25–30} seem to have mainly been performed in the ‘safe’ region $D < 0.5$, and systematic errors exceeding a few percent should be rare.

CIDEP Experiments.—Finally, we briefly consider the evaluation of CIDEP data from modulated e.s.r. experiments, since the correctness of one of our previous studies⁷ in that field has been doubted.⁴ Basically, if an ensemble of reactive radicals experiences electron spin polarizations at the stage of radical initiation and/or during F-pair encounters, the dynamics of the magnetization is determined not only by the chemical reaction kinetics but also by the dynamics of the spin polarizing and depolarizing processes. It has been shown⁷ that in modulation experiments this additional dynamics can be accounted for in form of an additional ‘polarization time constant’ τ_p , yielding equation (39) for the total phase lag Φ of the magnetization. τ_p

$$\Phi = \psi_R + \arctan(\omega\tau_p) \quad (39)$$

is given by equation (40). It depends on the relaxation time T_1 ,

$$\tau_p = T_1 p^I \left[1 + \frac{T_1}{\tau} (p^I + p^F) \right]^{-1} \quad (40)$$

the second-order radical lifetime τ , and the polarizations p^I and p^F developed in the radical initiation process and during F-pair encounters, respectively. The usual way to determine τ and τ_p is to plot $\omega/\tan\Phi$ versus ω^2 . Because of equations (39) and (29) this yields a linear relation (41) and the time constants are easily

$$\frac{\omega}{\tan\Phi} = \frac{1}{\tau_p - \tau} (1 + \tau\tau_p\omega^2) \quad (41)$$

obtained from the intercept and slope.

As before, relation (41) is strictly valid only for a homogeneous radical distribution. Taking into account the Beer–Lambert law, by properly averaging the relevant equations in ref. 7, equation (41) is replaced by (42) where equations (43) and

$$\tan\bar{\Phi} = \frac{X + 2\omega\tau T_1 p^F Y}{\omega T_1 p^F X - 2Y - T_1(1 - e^{-\alpha})(p^I + p^F)/\tau_0} \quad (42)$$

$$X = \omega\tau_0 \left[\alpha - \ln \left(\frac{1 + \omega^2\tau_0^2 e^\alpha}{1 + \omega^2\tau_0^2} \right) \right] \quad (43)$$

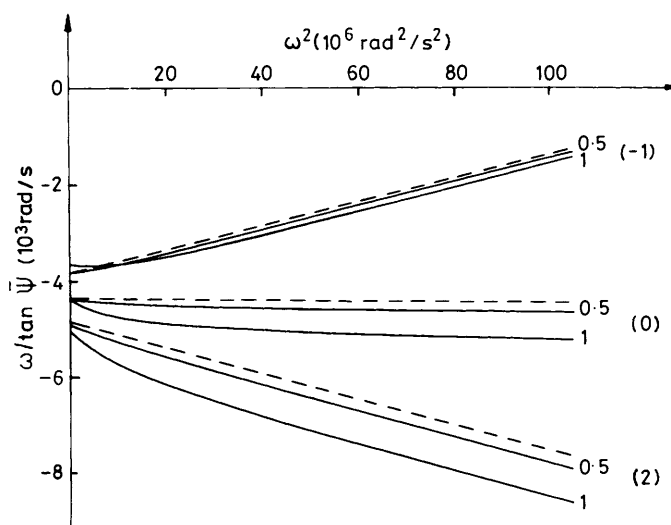


Figure 8. Frequency dependences of the phase lag ψ of magnetizations for three hyperfine states ($-1, 0, 2$) of 1-hydroxy-1-methylethyl radicals during photoreduction of acetone with propan-2-ol.⁷ Broken lines refer to a uniform concentration, full lines are calculated from equations (42) for absorbances $D = 0.5$ and 1

Table 4. Second-order and ‘polarization’ lifetimes $\bar{\tau}^F$ and $\bar{\tau}_p^F$ from fits of $\Phi(\omega)$ to equation (41) for various absorbances and three hyperfine transitions of 1-hydroxy-1-methylethyl radicals⁷ compared with the correct values $\bar{\tau}$ and τ_p

D	Line	$\bar{\tau}/\mu\text{s}$	$\bar{\tau}^F/\mu\text{s}$	$\bar{\tau}_p/\mu\text{s}$	$\bar{\tau}_p^F/\mu\text{s}$
0.2	-1	230	230	-28.0	-27.9
	0	230	229	1.4	1.6
	2	230	229	24.1	24.2
0.5	-1	230	229	-28.0	-27.4
	0	230	227	1.4	2.2
	2	230	224	24.1	24.8
1.0	-1	230	228	-28.0	-26.2
	0	230	218	1.4	5.3
	2	230	208	24.1	26.7

(44) hold and, according to equation (17), we have (45).

$$Y = 1 - e^{-\alpha/2} + \omega\tau_0 \arctan \frac{\omega\tau_0(1 - e^{-\alpha/2})}{1 + \omega^2\tau_0^2 e^{\alpha/2}} \quad (44)$$

$$\tau_0 = \frac{2}{\alpha} (1 - e^{-\alpha/2}) \bar{\tau} \quad (45)$$

In Figure 8 the correct frequency dependence of $\bar{\Phi}$ [equation (42) full lines] is compared with relation (41) (broken lines). Comparison is made for two absorbances, $D = 0.5$ and 1.0 , and for three resonance lines (labelled with $-1, 0$, and 2) of the 1-hydroxy-1-methylethyl radical, which have been analysed in our previous work.⁷ Obviously, while the emissive line (-1) is only weakly affected by the inhomogeneity effect, the deviations are more pronounced for the nearly unpolarized line (0) and the enhanced absorption resonance (2). Table 4 compares the ‘correct’ time constants $\bar{\tau}$ and $\bar{\tau}_p$,⁷ which have been used to calculate $\bar{\Phi}(\omega)$, with the parameters $\bar{\tau}^F$ and $\bar{\tau}_p^F$, resulting from ‘forced’ linear fits according to equation (41). Values for $D = 0.2$ are also included, since that was the average optical density in our previous measurements.⁷ Several conclusions can be drawn from the data in Table 4.

(a) At high absorbances, neglect of the Beer–Lambert law in

the evaluation of spin-polarized radical systems leads to different chemical lifetimes $\bar{\tau}^F$ for differently polarized states. While $\bar{\tau}^F$ of enhanced absorption lines is shortened, there is nearly no effect on $\bar{\tau}^F$ for emission lines ($\bar{\tau}_p < 0$).

(b) Neglect of the Beer-Lambert law introduces nearly no error in $\bar{\tau}_p^F$ for strongly emissive lines, a slightly larger one for strong enhanced absorption lines, and a large relative error in $\bar{\tau}_p^F$ for nearly unpolarized transitions (line 0).

(c) The simple evaluation according to equation (41) supplies rather reliable values for $\bar{\tau}$ and $\bar{\tau}_p$ as long as $D < 0.5$.

(d) All kinetic and CIDEP data given in our previous work⁷ are correct within their statistical error limits.

Concluding Remarks.—The theoretical analyses and their experimental verifications presented here for the effects of non-uniform radical concentration distributions caused by photochemical radical generation on the kinetic interpretation of time- or phase-resolving experimental results clearly invalidate previous statements of Basu and McLauchlan.⁴ If they had been correct a wealth of accumulated data on second-order radical reactions³ would now be obsolete. Fortunately, the effects are generally small unless rather high absorbances are used. For these they can easily be taken into account by application of the proper formulas and correction factors given in this work. We appreciate, though, that the previous authors⁴ were first to state the problem to a wider audience.

Acknowledgements

We gratefully acknowledge communication of results⁶ prior to publication by Dr. R. Leuschner and Professor J. Dohrmann, Berlin, and financial support by the Swiss National Foundation for Scientific Research.

References

- 1 D. Griller and K. U. Ingold, *Acc. Chem. Res.*, 1980, **13**, 193.
- 2 P. Neta, *Adv. Phys. Org. Chem.*, 1976, **12**, 223.
- 3 For a recent compilation, see Landolt-Börnstein, 'Radical Reaction Rates in Liquids,' Springer, Berlin, 1983—1984, New Series, vols. II/13a—e.

- 4 S. Basu and K. A. McLauchlan, *J. Chem. Soc., Perkin Trans. 2*, 1983, 855.
- 5 R. Leuschner and J. K. Dohrmann, 2. Diskussionstagung, Fachgruppe Magn. Resonanz der GdCh, Königstein, 1980.
- 6 R. Leuschner, H. Krohn, and J. K. Dohrmann, *Ber. Bunsenges. Phys. Chem.*, 1984, **88**, 462.
- 7 H. Paul, *Chem. Phys.*, 1979, **40**, 265.
- 8 H. R. Dütsch and H. Fischer, *Int. J. Chem. Kinet.*, 1981, **13**, 527; 1982, **14**, 195.
- 9 M. Lehni and H. Fischer, *Int. J. Chem. Kinet.*, 1983, **15**, 733.
- 10 H. G. Korth, P. Lommès, W. Sicking, and R. Sustmann, *Int. J. Chem. Kinet.*, 1983, **15**, 267.
- 11 P. B. Ayscough and G. Lambert, *J. Chem. Soc., Faraday Trans. 1*, 1978, **74**, 2481.
- 12 K. Adamic, D. F. Bowman, T. Gillan, and K. U. Ingold, *J. Am. Chem. Soc.*, 1971, **93**, 902.
- 13 R. W. Dennis and B. P. Roberts, *J. Chem. Soc., Perkin Trans. 2*, 1975, 140.
- 14 S. K. Wong, W. Sytnyk, and J. K. S. Wan, *Can. J. Chem.*, 1972, **50**, 3052.
- 15 P. B. Ayscough and M. C. Brice, *J. Chem. Soc. B*, 1971, 491.
- 16 S. K. Wong, *Int. J. Chem. Kinet.*, 1981, **13**, 433.
- 17 K. Münger and H. Fischer, *Int. J. Chem. Kinet.*, 1984, **16**, 1213.
- 18 H. Schuh and H. Fischer, *Int. J. Chem. Kinet.*, 1976, **8**, 341; *Helv. Chim. Acta*, 1978, **61**, 2130, 2463.
- 19 T. Kaiser, L. Grossi, and H. Fischer, *Helv. Chim. Acta*, 1978, **61**, 223.
- 20 M. Lehni, H. Schuh, and H. Fischer, *Int. J. Chem. Kinet.*, 1979, **11**, 705.
- 21 J. Lipscher and H. Fischer, *J. Phys. Chem.*, 1984, **88**, 2555.
- 22 Wu, Lung-min and H. Fischer, *Int. J. Chem. Kinet.*, in the press.
- 23 G. B. Watts and K. U. Ingold, *J. Am. Chem. Soc.*, 1972, **94**, 491.
- 24 P. Schmid, D. Griller, and K. U. Ingold, *Int. J. Chem. Kinet.*, 1979, **11**, 333.
- 25 T. J. Burkey and D. Griller, *Rev. Chem. Intermed.*, 1984, **5**, and references cited therein.
- 26 H. Paul, *Chem. Phys.*, 1976, **15**, 115.
- 27 C. Huggenberger and H. Fischer, *Helv. Chim. Acta*, 1981, **64**, 338.
- 28 R. F. Claridge and H. Fischer, *J. Phys. Chem.*, 1983, **87**, 1960.
- 29 H. Paul, R. D. Small, and J. C. Scaiano, *J. Am. Chem. Soc.*, 1978, **100**, 4520.
- 30 H. Paul, *J. Phys. Chem.*, 1978, **82**, 2754.

Received 26th March 1984; Paper 4/484